

Extended orbital resonance model with hump-induced oscillations

Zdeněk Stuchlík^a, Petr Slaný and Gabriel Török

Institute of Physics, Faculty of Philosophy & Science, Silesian University in Opava,
 Bezručovo nám. 13, CZ-746 01 Opava, Czech Republic

^azdenek.stuchlik@fpf.slu.cz

ABSTRACT

Change of sign of the LNRF-velocity gradient has been found for accretion discs orbiting rapidly rotating Kerr black holes with spin $a > 0.9953$ for Keplerian discs and $a > 0.99979$ for marginally stable thick discs. Such a “humpy” LNRF-velocity profiles occur just above the marginally stable circular geodesic and could be related to oscillations of accretion discs. The frequency of such “hump”-induced oscillations can be identified with the maximal rate of change of the orbital velocity within the “humpy” profile. Therefore, we introduce an extended orbital resonance model (EXORM) of quasiperiodic oscillations (QPOs) assuming non-linear resonant phenomena between oscillations with the orbital epicyclic frequencies and the humpy frequency defined in a fully general relativistic way. The EXORM is developed for both Keplerian discs and perfect-fluid tori where the approximation of oscillations with epicyclic frequencies is acceptable. Clearly, the EXORM could be applied to the near-extreme Kerr black hole systems exhibiting relatively complex QPO frequency patterns. Assuming a Keplerian disc, it can be shown that in the framework of the EXORM, all the QPOs observed in the microquasar GRS 1915+105 could be explained, while it is not possible in the case of QPOs observed in the Galactic Centre source Sgr A*.

Keywords: Black hole physics – accretion, accretion disks – relativity

1 INTRODUCTION

High frequency (kHz) twin peak quasi-periodic oscillations (QPOs) with frequency ratios 3 : 2 (and sometimes 3:1) are observed in microquasars (see, e.g., van der Klis, 2000; McClintock and Remillard, 2004; Remillard, 2005). In the Galactic Centre black hole Sgr A*, Genzel et al. (2003) measured a clear periodicity of 1020 sec in variability during a flaring event. This period is in the range of Keplerian orbital periods at a few gravitational radii from a black hole with mass $M \sim 3.6 \times 10^6 M_\odot$ estimated for Sgr A* (Ghez et al., 2005; Weinberg et al., 2005). More recently, Aschenbach et al. (2004); Aschenbach (2004, 2006) reported three QPO periodicities at 692 sec, 1130 sec and 2178 sec that correspond to frequency

ratios $(1/692):(1/1130):(1/2178) \sim 3:2:1$. These observational data are not quite convincing (see, e.g., Abramowicz et al., 2004), but surely deserve attention (Aschenbach, 2007).

Detailed analysis of the variable X-ray black-hole binary system (microquasar) GRS 1915+105 reveals high-frequency QPOs appearing at five frequencies, namely $\nu_1 = (27 \pm 1)$ Hz (Belloni et al., 2001), $\nu_2 = (41 \pm 1)$ Hz, $\nu_3 = (67 \pm 1)$ Hz (Morgan et al., 1997; Strohmayer, 2001), and $\nu_4 = (113 \pm 5)$ Hz, $\nu_5 = (167 \pm 5)$ Hz (Remillard and McClintock, 2006). In this range of their errors, both upper pairs are close to the frequency ratio $3:2$ suggesting the possible existence of resonant phenomena in the system. Observations of oscillations with these frequencies have different qualities, but in all five cases the data are quite convincing (see McClintock and Remillard, 2004; Remillard and McClintock, 2006).

Several models have been developed to explain the kHz QPO frequencies, and it is usually preferred that these oscillations are related to the orbital motion near the inner edge of an accretion disc. In particular, two ideas based on the strong-gravity properties have been proposed. While Stella and Vietri (1998, 1999) introduced the “Relativistic Precession Model” considering that the kHz QPOs directly manifest the modes of a slightly perturbed (and therefore epicyclic) relativistic motion of blobs in the inner parts of the accretion disc, Kluźniak and Abramowicz (2001) propose models based on non-linear oscillations of an accretion disc that assume resonant interaction between orbital and/or epicyclic modes. In a different context, the possibility of resonant coupling between the epicyclic modes of motion in the Kerr spacetime was also mentioned in the early work of Aliev and Galtsov (1981). The radial and vertical epicyclic oscillations could be related to both the thin Keplerian discs (Abramowicz et al., 2003; Kato, 2001) and the thick, toroidal accretion discs (Rezzolla et al., 2003). In particular, the observations of high frequency twin peak QPOs with the $3:2$ frequency ratio in microquasars can be explained by the parametric resonance between the radial and vertical epicyclic oscillations, $\nu_v:\nu_r \sim 3:2$. This hypothesis, under the assumption of geodesic oscillations (i.e., for thin discs), puts strong limit on the mass-spin relation for the central black hole in microquasars (Török et al., 2005; Török, 2005; Török et al., 2006).

Aschenbach (2004, 2006, 2007) discovered that two changes of sign of the radial gradient of the Keplerian orbital velocity as measured in the locally non-rotating frame (LNRF, Bardeen et al., 1972) occur in the equatorial plane of Kerr black holes with $a > 0.9953$. Stuchlík et al. (2005) have found that the gradient sign change in the LNRF-velocity profiles occurs also for non-geodesic motion with uniform distribution of the specific angular momentum $\ell(r, \theta) = \text{const}$ (i.e., in marginally stable thick discs) around extremely rapid Kerr black holes with $a > 0.99979$.¹ The global character of the phenomenon is given in terms of topology changes of the von Zeipel surfaces (equivalent to equipotential surfaces in the tori with $\ell(r, \theta) = \text{const}$).

¹ Note that the assumption of uniform distribution of the specific angular momentum can be relevant at least at the inner parts of the thick disc and that matter in the disc follows nearly geodesic circular orbits nearby the center of the disc and in the vicinity of its inner edge determined by the cusp of its critical equipotential surface (see Abramowicz et al., 1978).

Toroidal von Zeipel surfaces exist around the circle corresponding to the minimum of the equatorial LNRF-velocity profile, indicating possibility of development of some instabilities in that part of the marginally stable disc with positive gradient of the orbital velocity in LNRF (Stuchlík et al., 2004, 2005, 2006a,b, 2007a,b,c,d).

The positive radial gradient of orbital LNRF-velocity around black holes with $a > 0.9953$ seems to be a physically interesting phenomenon, even if a direct mechanism relating this phenomenon to triggering the oscillations, and subsequent linking of the oscillations to the excitation of radial (and vertical) epicyclic oscillations, is unknown. Therefore, an extended orbital resonance model (EXORM) has been developed, with hypothetical hump-induced oscillations assumed to enter a non-linear resonance with the radial or vertical epicyclic oscillations (Stuchlík et al., 2007b). It should be stressed that due to the non-linear resonance, combinational frequencies are allowed to be observable.

In the EXORM, the frequency of the hump-induced oscillations is related to the maximal positive radial gradient of the LNRF-velocity in the “humpy” velocity profile in the general relativistic, coordinate-independent form. Further, since the gradient is defined locally, being connected to the LNRF, it has to be transformed into the form related to distant stationary observers, giving observationally relevant “humpy” frequency ν_h . Then the “humpy” and epicyclic frequencies could be estimated at the radius of definition of the “humpy” frequency.

In the case of Keplerian discs, the epicyclic resonance radii $r_{3:1}$ and $r_{4:1}$ (with $\nu_v:\nu_r = 3:1, 4:1$) are located in vicinity of the “humpy” radius r_h where efficient triggering of oscillations with frequencies $\sim \nu_h$ could be expected. Asymptotically (for $1 - a < 10^{-4}$) the ratio of the epicyclic and Keplerian frequencies and the humpy frequency is nearly constant, i.e., almost independent of a , being for the radial epicyclic frequency $\nu_r:\nu_h \sim 3:2$. In the case of thick discs, the situation is more complex due to dependence on distribution of the specific angular momentum ℓ determining the disc properties. For $1 - a < 10^{-6}$, the frequency ratios of the humpy frequency and the orbital and epicyclic frequencies are again nearly constant and independent of both a and ℓ being for the radial epicyclic frequency $\nu_r:\nu_h \sim 4:1$. In the limiting case of very slender tori ($\ell \sim \ell_{ms}$) the epicyclic resonance radius $r_{4:1} \sim r_h$ for all the relevant interval of $1 - a < 2 \times 10^{-4}$.

In Section 2, we briefly summarize properties of the Aschenbach effect for Keplerian thin discs, and $\ell = \text{const}$ thick discs. In Section 3, the extended resonance model is introduced, i.e., the critical “humpy” frequency, connected to the LNRF-velocity positive gradient in the humpy profiles, is given in the physically relevant, coordinate independent form for the both Keplerian and $\ell = \text{const}$ discs. At the radius of its definition, the humpy frequency is compared to the radial and vertical epicyclic frequency and the orbital frequency. In Section 4, fitting of the observed frequencies in the GRS 1915+105 microquasar in the framework of the EXORM is summarized, while it is demonstrated that the data reported for Sgr A* could not be probably fitted by EXORM. In Section 5, concluding remarks are presented.

2 LNRF-VELOCITY PROFILES OF ACCRETION DISCS

The locally non-rotating frames (LNRF) are given by the tetrad of 1-forms (Bardeen et al., 1972)

$$\begin{aligned} e^{(t)} &= \left(\frac{\Sigma \Delta}{A} \right)^{1/2} dt, & e^{(\varphi)} &= \left(\frac{A}{\Sigma} \right)^{1/2} \sin \theta (d\varphi - \omega dt), \\ e^{(r)} &= \left(\frac{\Sigma}{\Delta} \right)^{1/2} dr, & e^{(\theta)} &= \Sigma^{1/2} d\theta, \end{aligned} \quad (1)$$

where

$$\omega = -\frac{g_{t\varphi}}{g_{\varphi\varphi}} = \frac{2ar}{A} \quad (2)$$

is the angular velocity of the LNRF relative to distant observers.

In the Kerr spacetimes with the rotational parameter assumed to be $a > 0$, the relevant metric coefficients in the standard Boyer–Lindquist coordinates read:

$$g_{tt} = -\frac{\Delta - a^2 \sin^2 \theta}{\Sigma}, \quad g_{t\varphi} = -\frac{2ar \sin^2 \theta}{\Sigma}, \quad g_{\varphi\varphi} = \frac{A \sin^2 \theta}{\Sigma}, \quad g_{rr} = \frac{\Sigma}{\Delta}, \quad g_{\theta\theta} = \Sigma, \quad (3)$$

where

$$\Delta = r^2 - 2r + a^2, \quad \Sigma = r^2 + a^2 \cos^2 \theta, \quad A = (r^2 + a^2)^2 - \Delta a^2 \sin^2 \theta. \quad (4)$$

The geometrical units, $c = G = 1$, together with putting the mass of the black hole $M = 1$, are used in order to obtain completely dimensionless formulae hereafter.

For matter orbiting a Kerr black hole with a 4-velocity U^μ and angular velocity profile $\Omega(r, \theta)$, the azimuthal component of its 3-velocity in the LNRF reads

$$\mathcal{V}^{(\varphi)} = \frac{U^\mu e_\mu^{(\varphi)}}{U^\nu e_\nu^{(t)}} = \frac{A \sin \theta}{\Sigma \sqrt{\Delta}} (\Omega - \omega). \quad (5)$$

2.1 Keplerian thin discs

In thin discs matter follows nearly circular geodetical orbits characterized by the Keplerian distributions of the angular velocity and the specific angular momentum (in the equatorial plane, $\theta = \pi/2$)

$$\Omega = \Omega_K(r; a) \equiv \frac{1}{(r^{3/2} + a)}, \quad \ell = \ell_K(r; a) \equiv \frac{r^2 - 2ar^{1/2} + a^2}{r^{3/2} - 2r^{1/2} + a}. \quad (6)$$

The azimuthal component of the Keplerian 3-velocity in the LNRF reads

$$\mathcal{V}_K^{(\varphi)}(r; a) = \frac{(r^2 + a^2)^2 - a^2 \Delta - 2ar(r^{3/2} + a)}{r^2(r^{3/2} + a)\sqrt{\Delta}} \quad (7)$$

and formally diverges for $r \rightarrow r_+ = 1 + \sqrt{1 - a^2}$, where the black-hole event horizon is located. Its radial gradient is given by

$$\frac{\partial \mathcal{V}_K^{(\varphi)}}{\partial r} = - \frac{r^5 + a^4(3r + 2) - 2a^3r^{1/2}(3r + 1) - 2a^2r^2(2r - 5) + 2ar^{5/2}(5r - 9)}{2\Delta^{3/2}\sqrt{r}(r^{3/2} + a)^2}. \quad (8)$$

As shown by Aschenbach (2004, 2006), the velocity profile has two changes of the gradient sign (where $\partial \mathcal{V}^{(\varphi)}/\partial r = 0$) in the field of rapidly rotating Kerr black holes with $a > a_{c(K)} \doteq 0.9953$.

2.2 Marginally stable tori

Perfect-fluid stationary and axisymmetric toroidal discs are characterized by the 4-velocity field $U^\mu = (U^t, 0, 0, U^\varphi)$ with $U^t = U^t(r, \theta)$, $U^\varphi = U^\varphi(r, \theta)$, and by distribution of the specific angular momentum $\ell = -U_\varphi/U_t$. The angular velocity of orbiting matter, $\Omega = U^\varphi/U^t$, is then related to ℓ by the formula

$$\Omega = - \frac{\ell g_{tt} + g_{t\varphi}}{\ell g_{t\varphi} + g_{\varphi\varphi}}. \quad (9)$$

The marginally stable tori are characterized by uniform distribution of the specific angular momentum

$$\ell = \ell(r, \theta) = \text{const}, \quad (10)$$

and are fully determined by the spacetime structure through equipotential surfaces of the potential $W = W(r, \theta)$ defined by the relations (Abramowicz et al., 1978)

$$W - W_{\text{in}} = \ln \frac{U_t}{(U_t)_{\text{in}}}, \quad (U_t)^2 = \frac{g_{t\varphi}^2 - g_{tt}g_{\varphi\varphi}}{g_{tt}\ell^2 + 2g_{t\varphi}\ell + g_{\varphi\varphi}}; \quad (11)$$

the subscript “in” refers to the inner edge of the disc. The LNRF orbital velocity of the torus is given by

$$\mathcal{V}_T^{(\varphi)} = \frac{A(\Delta - a^2 \sin^2 \theta) + 4a^2 r^2 \sin^2 \theta}{\Sigma \sqrt{\Delta} (A - 2a\ell r) \sin \theta} \ell. \quad (12)$$

For marginally stable tori it is enough to consider the motion in the equatorial plane, $\theta = \pi/2$. Formally, this velocity vanishes for $r \rightarrow \infty$ and $r \rightarrow r_+$, i.e., there must be a change of its radial gradient for any values of the parameters a and ℓ , contrary to the case of Keplerian discs. The radial gradient of the equatorial LNRF velocity of $\ell = \text{const}$ tori reads

$$\begin{aligned} \frac{\partial \mathcal{V}_T^{(\varphi)}}{\partial r} = & \left\{ \frac{[\Delta + (r - 1)r][r(r^2 + a^2) - 2a(\ell - a)]}{[r(r^2 + a^2) - 2a(\ell - a)]^2 \sqrt{\Delta}} \right. \\ & \left. - \frac{r(3r^2 + a^2)\Delta}{[r(r^2 + a^2) - 2a(\ell - a)]^2 \sqrt{\Delta}} \right\} \ell, \end{aligned} \quad (13)$$

so it changes its orientation at radii determined for a given ℓ by the condition

$$\ell = \ell_{\text{ex}}(r; a) \equiv a + \frac{r^2[(r^2 + a^2)(r - 1) - 2r\Delta]}{2a[\Delta + r(r - 1)]}. \quad (14)$$

For both thick tori and Keplerian discs we have to consider the limit on the disc extension given by the innermost stable orbit. For Keplerian discs this is the marginally stable geodetical orbit, $r_{\text{in}} \approx r_{\text{ms}}$, while for thick tori this is an unstable circular geodesic kept stable by pressure gradients and located between the marginally bound and the marginally stable geodetical orbits, $r_{\text{mb}} \lesssim r_{\text{in}} \lesssim r_{\text{ms}}$, with the radius being determined by the specific angular momentum $\ell = \text{const} \in (\ell_{\text{ms}}, \ell_{\text{mb}})$ through the equation $\ell = \ell_{\text{K}}(r; a)$; ℓ_{ms} (ℓ_{mb}) denotes specific angular momentum of the circular marginally stable (marginally bound) geodesic.

Detailed discussion of Stuchlík et al. (2005) shows that two physically relevant changes of sign of $\partial \mathcal{V}_{\text{T}}^{(\varphi)} / \partial r$ in the tori occur for Kerr black holes with the rotational parameter $a > a_{\text{c(T)}} \doteq 0.99979$. The interval of relevant values of the specific angular momentum $\ell \in (\ell_{\text{ms}}(a), \ell_{\text{ex(max)}}(a))$, where $\ell_{\text{ex(max)}}(a)$ corresponds to the local maximum of the function (14), grows with a growing up to the critical value of $a_{\text{c(mb)}} \doteq 0.99998$. For $a > a_{\text{c(mb)}}$, the interval of relevant values of $\ell \in (\ell_{\text{ms}}(a), \ell_{\text{mb}}(a))$ is narrowing with the rotational parameter growing up to $a = 1$, which corresponds to a singular case where $\ell_{\text{ms}}(a = 1) = \ell_{\text{mb}}(a = 1) = 2$. Notice that the situation becomes to be singular only in terms of the specific angular momentum; it is shown (see Bardeen et al., 1972) that for $a = 1$ both the total energy E and the axial angular momentum L differ at r_{ms} and r_{mb} , respectively, but their combination, $\ell \equiv L/E$, giving the specific angular momentum, coincides at these radii.

A physically reasonable global quantity characterizing rotating fluid configurations in terms of the LNRF orbital velocity is so-called von Zeipel radius defined by the relation

$$\mathcal{R} \equiv \frac{\ell}{\mathcal{V}_{\text{LNRF}}^{(\varphi)}} = (1 - \omega\ell) \tilde{\varrho}, \quad (15)$$

which generalizes in another way as compared with (Abramowicz et al., 1995) the Schwarzschildian definition of the gyration radius $\tilde{\varrho}$ (Abramowicz et al., 1993). Note that, except for the Schwarzschild case $a = 0$, the von Zeipel surfaces, defined as the surfaces of $\mathcal{R}(r, \theta; a, \ell) = \text{const}$, *do not coincide* with those introduced by Kozłowski et al. (1978) as the surfaces of constant ℓ/Ω (see Stuchlík et al., 2005 for more details).

In the case of marginally stable tori the von Zeipel surfaces $\mathcal{R} = \text{const}$ coincide with the equivelocity surfaces $\mathcal{V}^{(\varphi)}(r, \theta; a, \ell) = \mathcal{V}_{\text{T}}^{(\varphi)} = \text{const}$. Topology of the von Zeipel surfaces can be directly determined by the behaviour of the von Zeipel radius in the equatorial plane

$$\mathcal{R}(r, \theta = \pi/2; a, \ell) = \frac{r(r^2 + a^2) - 2a(\ell - a)}{r\sqrt{\Delta}}. \quad (16)$$

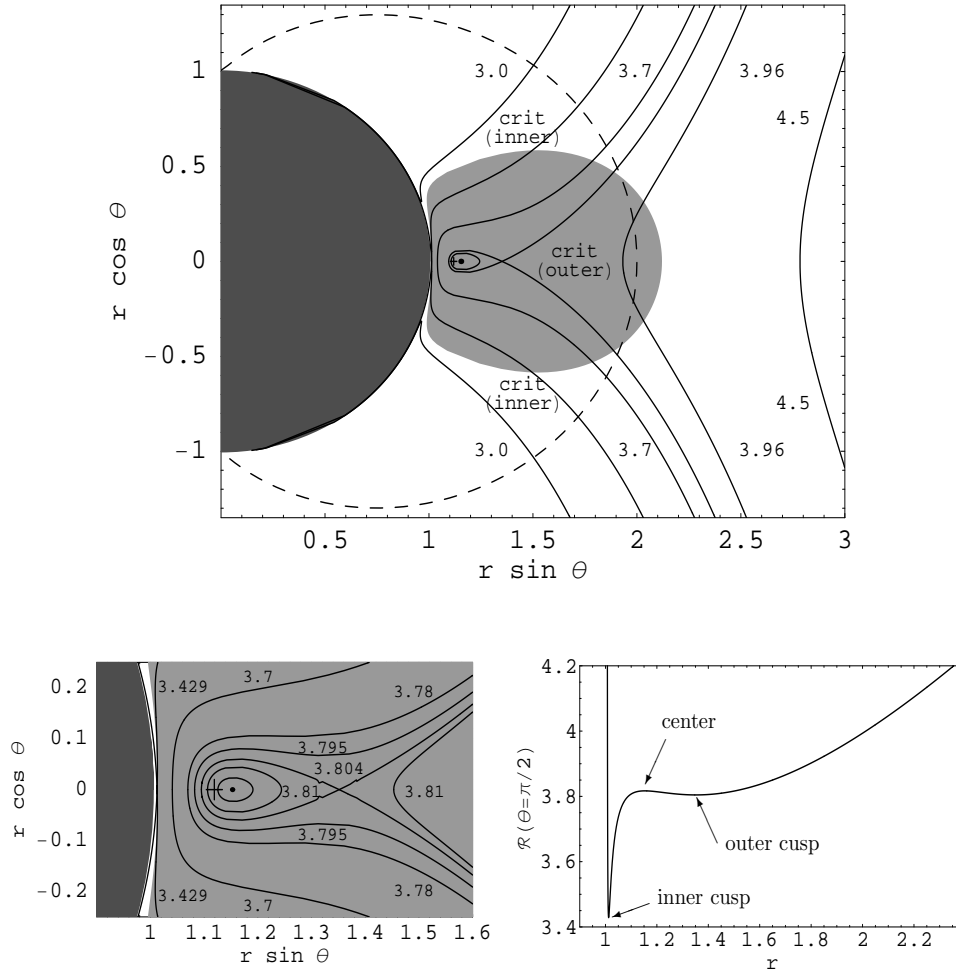


Figure 1. Von Zeipel surfaces (meridional sections). For $a > a_{c(T)}$ and ℓ appropriately chosen, two surfaces with a cusp, or one surface with both the cusps, together with closed (toroidal) surfaces, exist, being located always inside the ergosphere (dashed surface) of a given spacetime. Both the outer cusp and the central ring of closed surfaces are located inside the toroidal equilibrium configurations corresponding to marginally stable thick discs (light-gray region; its shape is determined by the critical self-crossing *equipotential surface* of the potential $W(r, \theta)$). The cross (+) denotes the centre of the torus. Dark region corresponds to the black hole. Figures illustrating all possible configurations of the von Zeipel surfaces are presented in Stuchlík et al. (2005). Here we present the figure plotted for the parameters $a = 0.99998$, $\ell = 2.0065$. Critical value of the von Zeipel radius corresponding to the inner and the outer self-crossing surface is $\mathcal{R}_{c(in)} \doteq 3.429$ and $\mathcal{R}_{c(out)} \doteq 3.804$, respectively, the central ring of toroidal surfaces corresponds to the value $\mathcal{R}_{center} \doteq 3.817$. Interesting region containing both the cusps and the toroidal surfaces is plotted in detail at the left lower figure. Right lower figure shows the behaviour of the von Zeipel radius in the equatorial plane. (Taken from Stuchlík et al., 2007b)

The local minima of the function (16) determine loci of the cusps of the von Zeipel surfaces, while its local maximum (if it exists) determines a circle around which closed toroidally shaped von Zeipel surfaces are concentrated (see Fig. 1). Notice that the inner cusp is always physically irrelevant being located outside of the toroidal configuration of perfect fluid. Behaviour of the von Zeipel surfaces nearby the centre and the inner edge of the thick discs orbiting Kerr black holes with $a > a_{c(T)} \doteq 0.99979$, i.e., the existence of the von Zeipel surface with toroidal topology, suggests possible generation of instabilities in both the vertical and radial direction.

In terms of the redefined rotational parameter $(1 - a)$, the “humpy” profile of the LNRF orbital velocity of marginally stable thick discs occurs for discs orbiting Kerr black holes with $1 - a < 1 - a_{c(T)} \doteq 2.1 \times 10^{-4}$, which is more than one order lower than the value $1 - a_{c(K)} \doteq 4.7 \times 10^{-3}$ found by Aschenbach (2004) for the Keplerian thin discs. Moreover, in the thick discs, the velocity difference $\Delta \mathcal{V}_T^{(\varphi)}$ is smaller but comparable with those in the thin discs. In fact, for $a \rightarrow 1$, the velocity difference in the thick discs $\Delta \mathcal{V}_T^{(\varphi)} \approx 0.02$, while for the Keplerian discs it goes even up to $\Delta \mathcal{V}_K^{(\varphi)} \approx 0.07$ (Stuchlík et al., 2007d).

3 EXTENDED ORBITAL RESONANCE MODEL

The orbital resonance model assumes non-linear parametric and forced resonances of oscillations with the orbital (Keplerian) and radial or vertical epicyclic frequencies, or their combinations. Here, we extend this model by introducing hypothetical additional oscillations, induced by the hump in the LNRF-velocity profile of accretion discs of both Keplerian and toroidal character, that are supposed to be in a non-linear resonance with orbital or epicyclic oscillations.

In Kerr spacetimes, the frequencies of the radial and latitudinal (vertical) epicyclic oscillations related to an equatorial Keplerian circular orbit at a given r are determined by the formulae (see, e.g., Aliev and Galtsov, 1981)

$$\nu_r^2 = \nu_K^2 (1 - 6r^{-1} + 8ar^{-3/2} - 3a^2r^{-2}), \quad (17)$$

$$\nu_v^2 \equiv \nu_\theta^2 = \nu_K^2 (1 - 4ar^{-3/2} + 3a^2r^{-2}), \quad (18)$$

where the Keplerian frequency $\nu_K = \Omega_K/2\pi$. A detailed analysis of properties of the epicyclic frequencies can be found in Török and Stuchlík (2005a,b). The epicyclic oscillations with the frequencies ν_r , ν_v can be related to both the thin Keplerian discs (Abramowicz and Kluźniak, 2001; Kato, 2004) and thick, toroidal discs (Rezzolla et al., 2003).

According to Aschenbach (2004, 2006), the non-monotonicity of the LNRF-velocity profile of accretion discs could excite oscillations with characteristic frequency that has to be related to the maximum gradient in the “humpy” part of the accretion discs velocity profile.

Although there is no detailed idea on the mechanism generating the hump-induced oscillations, it is clear that the Aschenbach proposal of defining the characteristic

frequency deserves attention. It should be stressed, however, that a detailed analysis of the instability could reveal a difference between the characteristic frequency and the actual observable one, as the latter should be associated with the fastest growing unstable mode. In any case, the humpy frequency represents an upper limit on the frequencies of the hump-induced oscillations, as it is given by maximum of the LNRF-velocity gradient in the humpy part of the velocity profile.

At the present state of the EXORM, we assume that the characteristic humpy frequency is a typical frequency of oscillations induced by the conjectured “humpy instability,” and that the humpy oscillations could excite oscillations with the epicyclic frequencies or some combinational frequencies, if appropriate conditions for a forced resonance are satisfied in vicinity of the radius where the humpy oscillations occur (Stuchlík et al., 2007d).

The fully general relativistic definition of the critical frequency for a possible excitation of oscillations in the disc is given by the relations

$$\nu_{\text{crit}}^{\tilde{R}} = \left. \frac{\partial \mathcal{V}^{(\varphi)}}{\partial \tilde{R}} \right|_{\text{max}}, \quad d\tilde{R} = \sqrt{g_{rr}} dr = \sqrt{\frac{\Sigma}{\Delta}} dr, \quad (19)$$

where $\mathcal{V}^{(\varphi)} = \mathcal{V}_{\text{K}}^{(\varphi)}(r; a)$ in thin Keplerian discs, and $\mathcal{V}^{(\varphi)} = \mathcal{V}_{\text{T}}^{(\varphi)}(r; l, a)$ in marginally stable thick discs and \tilde{R} is the physically relevant, coordinate independent proper radial distance. Such a locally defined frequency, confined naturally to the observers orbiting the black hole with the LNRF, should be further related to distant stationary observers by the formula (taken at the BL coordinate r corresponding to $(\partial \mathcal{V}^{(\varphi)} / \partial \tilde{R})_{\text{max}}$)

$$\nu_{\text{h}} = \nu_{\infty}^{\tilde{R}} = \sqrt{-(g_{tt} + 2\omega g_{t\varphi} + \omega^2 g_{\varphi\varphi})} \nu_{\text{crit}}^{\tilde{R}}. \quad (20)$$

We call such a coordinate-independent and, in principle, observable frequency the “humpy frequency,” as it is related to the humpy profile of $\mathcal{V}^{(\varphi)}$, and denote it ν_{h} . It should be stressed that the physically relevant humpy frequency $\nu_{\text{h}} = \nu_{\infty}^{\tilde{R}}$, connected to observations by distant observers and exactly defined by Eqs (19) and (20), represents an upper limit on characteristic frequencies of oscillations induced by the hump of the LNRF-velocity profile, and the realistic humpy frequencies, as observed by distant observers, can be expected close to but smaller than $\nu_{\infty}^{\tilde{R}}$. Further, we denote r_{h} the BL radius of definition of the humpy oscillations frequency, where $\partial \mathcal{V}^{(\varphi)} / \partial \tilde{R} = (\partial \mathcal{V}^{(\varphi)} / \partial \tilde{R})_{\text{max}}$.

In the case of the Keplerian discs we obtain the “humpy frequency” to be given by the relation

$$\begin{aligned} \nu_{\text{h}} = & \frac{-r_{\text{h}}^5 - a^4(3r_{\text{h}} + 2) + 2a^3r_{\text{h}}^{1/2}(3r_{\text{h}} + 1) - 2a^2r_{\text{h}}^2(2r_{\text{h}} - 5) + 2ar_{\text{h}}^{5/2}(5r_{\text{h}} - 9)}{2\Delta_{\text{h}}r_{\text{h}}^2(r_{\text{h}}^{3/2} + a)^2} \\ & \times \sqrt{r_{\text{h}} - 2 - \frac{4a^2}{r_{\text{h}}(r_{\text{h}}^2 + a^2) + 2a^2}}, \end{aligned} \quad (21)$$

where $\Delta_h = r_h^2 - 2r_h + a^2$. The BL radius r_h where the positive gradient of the velocity profile in terms of the proper radial distance reaches its maximum, so-called “humpy radius,” is given by the condition

$$\frac{\partial}{\partial r} \left(\frac{\partial \mathcal{V}^{(\varphi)}}{\partial \bar{r}} \right) = 0 \quad (22)$$

leading to the equation

$$\begin{aligned} 3a^7(r+2) + a^6\sqrt{r}(21r^2 + 18r - 4) - a^5r(33r^2 + 10r + 20) \\ + a^4r\sqrt{r}(45r^3 - 62r^2 - 68r + 16) - a^3r^3(83r^2 - 122r - 60) \\ + a^2r^4\sqrt{r}(27r^2 - 130r + 136) - 9ar^5(7r^2 - 26r + 24) \\ + r^7\sqrt{r}(3r - 2) = 0, \end{aligned} \quad (23)$$

which must be solved numerically. The spin dependence of the humpy radius and the related humpy frequency is illustrated in Fig. 2. The humpy radius r_h falls monotonically with increasing spin a , while the humpy frequency ν_h has a maximum for $a = 0.9998$, where $\nu_{h(\max)} = 607 (M_\odot/M) \text{ Hz}$, and it tends to $\nu_{h(a \rightarrow 1)} = 588 (M_\odot/M) \text{ Hz}$.

The ratios of the humpy frequency and the orbital and epicyclic frequencies at the humpy radius were determined in Stuchlík et al. (2007b) revealing almost spin-independent asymptotic behaviour for $a \rightarrow 1$ represented closely by the ratios of integer numbers, $\nu_K : \nu_\nu : \nu_r : \nu_h \sim 46 : 11 : 3 : 2$, which imply a possibility of resonant phenomena between the hump-induced and orbital or epicyclic oscillations. For Keplerian discs, the ratios of the epicyclic frequencies and the humpy frequency are given in the dependence on the black-hole spin in Fig. 3.

The marginally stable tori have a structure that depends on the value of the specific angular momentum $\ell \in (\ell_{\text{ms}}, \ell_{\text{mb}})$. The oscillations of slender tori ($\ell \approx \ell_{\text{ms}}$) have frequencies equal to the epicyclic frequencies relevant for test particle motion, but the frequencies of non-slender tori are different, as shown for pseudo-Newtonian tori (Šrámková, 2005; Blaes et al., 2007) and expected for tori in the strong gravitational field of Kerr black holes. Therefore, comparison of the humpy frequencies and the epicyclic frequencies is relevant for the slender tori only.

The humpy frequency is defined for all $a > 0.99979$ and all $\ell \in (\ell_{\text{ms}}, \ell_{\text{mb}})$, see Fig. 4. It is important that in the field of Kerr black holes with $1 - a < 10^{-8}$, there is $\nu_h(a, \ell) \simeq 150 \text{ Hz } (M/M_\odot)^{-1}$ independently of a and ℓ (Stuchlík et al., 2007b). Further, the physically important case of tori admitting evolution of toroidal von Zeipel surfaces with the critical surface self-crossing in both the inner and the outer cusps is allowed at $\ell = \ell_{\text{crit}}$, where $\ell_{\text{crit}} \gtrsim \ell_{\text{ms}}$ only slightly differs from ℓ_{ms} , i.e., such tori can be slender, see Fig. 4. The ratios of ν_r/ν_h , ν_ν/ν_h and ν_o/ν_h are given for the tori with $\ell \approx \ell_{\text{ms}}$ in Fig. 5. Their asymptotical values, valid for $1 - a < 10^{-6}$, are independent of both a and ℓ .

Of course, in realistic situations the hump-induced oscillation mechanism could work at the vicinity of r_h , with slightly different frequencies; we should take into account that the shift of the radius, where the mechanism works, shifts both the

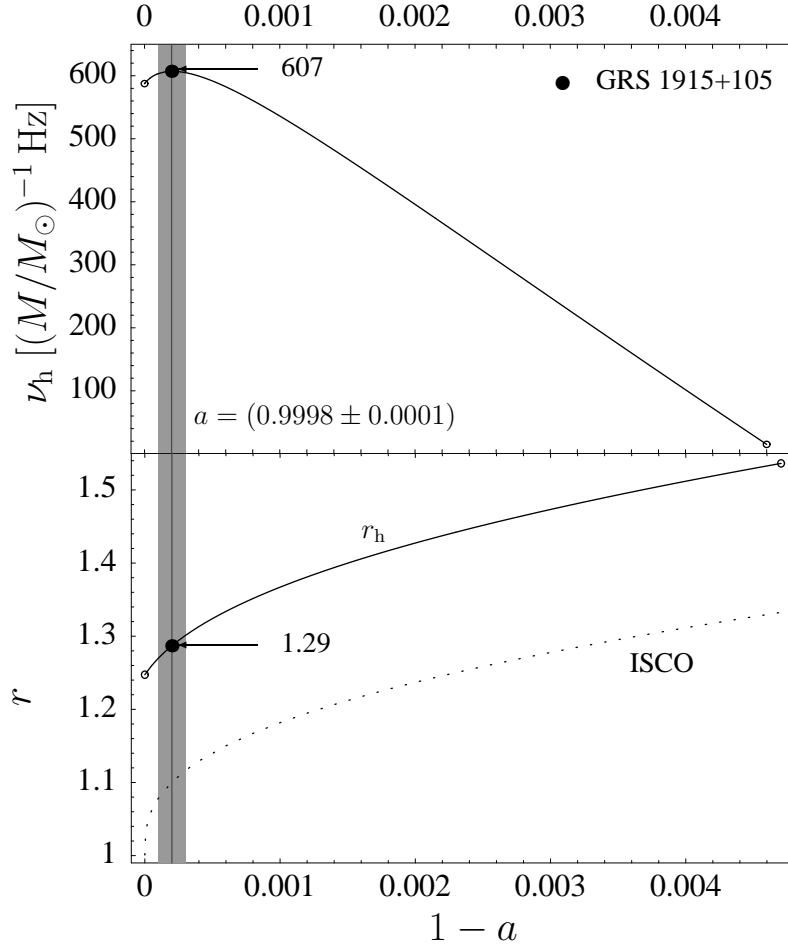


Figure 2. Spin-dependence of the humpy frequency ν_h and the humpy radius r_h that is compared with the Boyer–Lindquist radius of the innermost stable circular orbit. (Taken from Stuchlík et al., 2007d)

locally measured (LNRF) frequency (Eq. (19)) and the frequency related to distant observers (Eq. (20)). The zones of radii, where the critical frequency $\nu_{\text{crit}}^{\tilde{R}}$ differs up to 1 %, 10 % and 20 % of its maximal value (given by $(\partial \mathcal{V}^{(\varphi)} / \partial \tilde{R})_{\text{max}}$) for thin (Keplerian) discs or 1 %, 5 % and 10 % of its maximum for marginally stable discs with $\ell = \ell_{\text{ms}}$, are given in Fig. 6. We can see (Fig. 6) that the resonant epicyclic frequencies radii $r_{3:1}$ and $r_{4:1}$ are located within the zone of the hump-induced oscillation mechanism in both thin discs and marginally stable tori.

In Keplerian discs the sign changes of the radial gradient of the orbital velocity in LNRF occur nearby the $r = r_{3:1}$ orbit (with $\nu_v : \nu_r = 3 : 1$), while in the

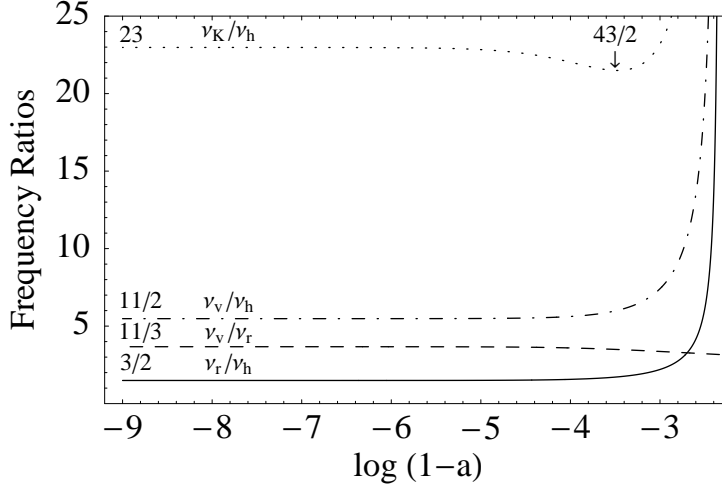


Figure 3. Spin dependence of the ratios of the radial (ν_r) and vertical (ν_v) epicyclic frequencies, and the Keplerian frequency (ν_K) to the thin-disc humpy frequency related to distant observers (ν_h). All the frequency ratios are asymptotically (for $1 - a < 10^{-4}$) constant. There is $\nu_K : \nu_v : \nu_r : \nu_h \sim 46 : 11 : 3 : 2$. Therefore, we can expect some resonant phenomena on the ratio of $\nu_r : \nu_h \sim 3 : 2$, and $\nu_K : \nu_v \sim 4$ that could be both correlated. (Taken from Stuchlík et al., 2007b)

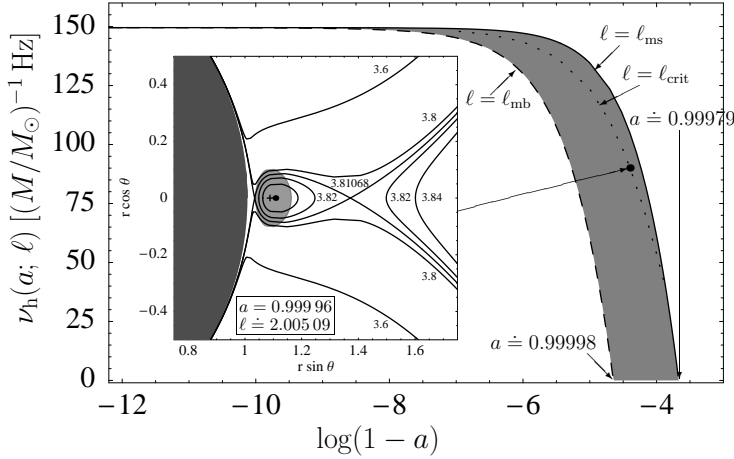


Figure 4. Interval of humpy frequencies for the marginally stable thick discs with $\ell \in (\ell_{ms}, \ell_{mb})$ as a function of the black-hole spin a . For $a \rightarrow 1$, the interval is narrowing and asymptotically reaching the value of $150 \text{ Hz } (M/M_\odot)^{-1}$. Dotted curve corresponds to the humpy frequencies of marginally stable slender tori with $\ell = \ell_{crit}$, for which the critical von Zeipel surface contains two cusps (as it is demonstrated for one special case in the left panel of the figure; the torus is given by the light-gray region).

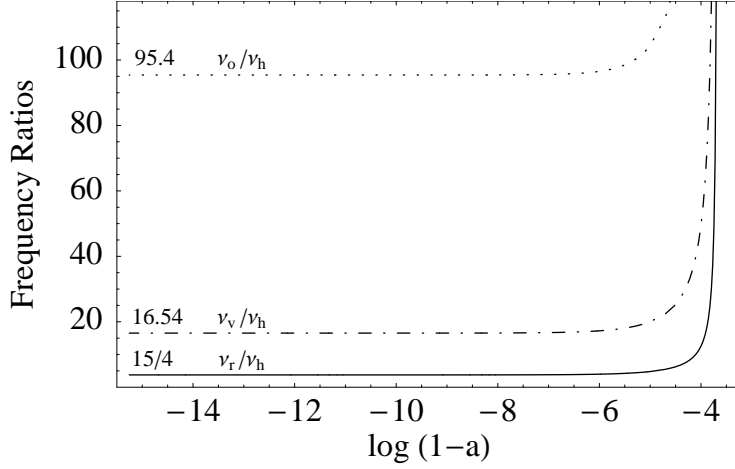


Figure 5. Spin dependence of the ratios of the radial (ν_r) and vertical (ν_v) epicyclic frequencies, and the orbital frequency (ν_o) of the marginally stable $\ell = \ell_{\text{ms}}$ disc to the thick-disc humpy frequency related to distant observers (ν_h). All the frequency ratios are asymptotically (for $1 - a < 10^{-6}$) almost constant. (Taken from Stuchlík et al., 2007b)

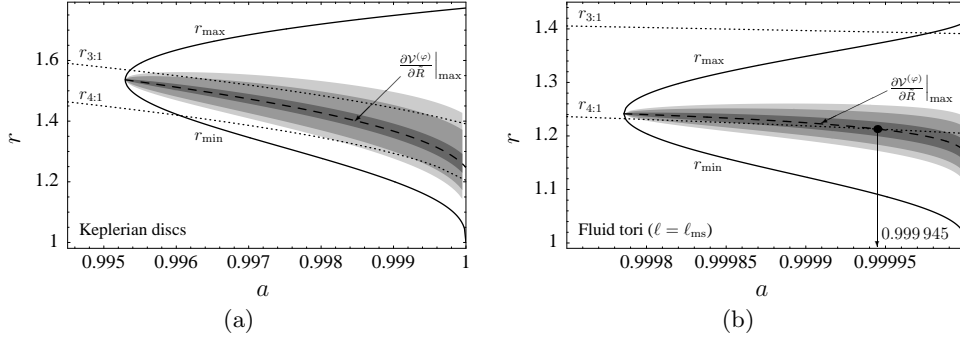


Figure 6. Positions of local extrema of $\mathcal{V}^{(\varphi)}$ (in BL coordinates) for Keplerian discs (a) and marginally stable discs with $\ell = \ell_{\text{ms}}$ (b) together with the locations of resonant orbits $r_{3:1}$ and $r_{4:1}$ (where the resonance between the vertical and radial epicyclic oscillations takes place) in dependence on the rotational parameter a of the black hole. Dashed curve corresponds to the maximum positive values of the LNRF orbital velocity gradient in terms of the proper radial distance where the critical frequency ν_{crit}^R is defined, boundaries of shaded regions correspond to orbits where the velocity gradient giving the characteristic frequency, $\partial\mathcal{V}^{(\varphi)}/\partial\tilde{R}$, reaches (a) 99%, 90%, 80% and (b) 99%, 95%, 90% of its maximum. (Taken from Stuchlík et al., 2007b)

vicinity of the $r = r_{3:2}$ orbit (with $\nu_v : \nu_r = 3 : 2$), $\partial\mathcal{V}^{(\varphi)}/\partial r < 0$ for all values of a for both Keplerian discs and marginally stable tori with all allowed values

of ℓ . The parametric resonance, which is the strongest one for the ratio of the epicyclic frequencies $\nu_v : \nu_r = 3 : 2$, can occur at the $r = r_{3:2}$ orbit, while its effect is much smaller at the radius $r = r_{3:1}$, as noticed by Abramowicz et al. (2003). Nevertheless, the forced resonance may take place at the $r_{3:1}$ orbit. Notice that the forced resonance at $r = r_{3:1}$ can generally result in observed QPOs frequencies with $3 : 2$ ratio due to the beat frequencies allowed for the forced resonance as shown in Abramowicz et al. (2004). But the forced resonance at $r_{3:1}$ between the epicyclic frequencies, induced by the humpy profile of $\mathcal{V}^{(\varphi)}$, seems to be irrelevant in the case of microquasars, since all observed frequencies lead to the values of the rotational parameter $a < a_{c(K)}$, as shown by Török et al. (2005).

4 APPLICATION OF THE EXTENDED RESONANCE MODEL

The extended orbital resonance model with hump-induced oscillations can be applied only to black hole systems containing a near-extreme Kerr black hole candidates. One of the most promising of such systems seems to be the microquasar GRS 1915+105, where the extremely high spin $a \sim 1$ was predicted by continuous spectra fitting method (McClintock et al., 2006). Another promising candidate for the near-extreme Kerr black hole could be considered the Galaxy Centre Sgr A*. In fact, all the QPO frequencies observed in GRS 1915+105 microquasar could be explained in the framework of the EXORM (Stuchlík et al., 2007d; Slaný and Stuchlík, 2007). Therefore, we briefly summarize these results, and then we consider the case of Sgr A*, assuming relevance of all the three frequencies reported by Aschenbach (Aschenbach, 2004, 2007).

4.1 GRS 1915+105

Assuming mass $M = 14.8 M_\odot$ and dimensionless spin $a = 0.9998$ for the GRS 1915+105 Kerr black hole (see Stuchlík et al., 2007d; Slaný and Stuchlík, 2007 for details), the EXORM predicts the following pattern of observable frequencies composed from the humpy and epicyclic frequencies and their combinations

$$\nu_1 \sim (\nu_r - \nu_h) = (26 \pm 2) \text{ Hz}, \quad (24)$$

$$\nu_h \equiv \nu_2 = (41 \pm 1) \text{ Hz}, \quad (25)$$

$$\nu_r \equiv \nu_3 = (67 \pm 1) \text{ Hz}, \quad (26)$$

$$\nu_4 \sim (\nu_r + \nu_h) = (108 \pm 2) \text{ Hz}, \quad (27)$$

$$\nu_5 \sim (\nu_v - \nu_r) = (0.17 \pm 0.01) \text{ kHz}. \quad (28)$$

The corresponding humpy radius is $r_h = 1.29$. At such a radius, the vertical epicyclic frequency of a particle orbiting the Kerr black hole with the mass and spin given above reaches the value $\nu_v = (0.23 \pm 0.01) \text{ kHz}$ that enters the highest (combinational) frequency.

4.2 Sgr A*

There are three frequencies related to the Sgr A* QPOs (Aschenbach, 2004; Török, 2005):

$$\nu_u = 1.445 \text{ mHz}, \quad \nu_m = 0.885 \text{ mHz}, \quad \nu_l = 0.459 \text{ mHz}. \quad (29)$$

These frequencies come in the rational ratio $\nu_u : \nu_m : \nu_l \sim 3:2:1$. Assuming EXORM with the humpy and radial epicyclic frequency and their combinational frequencies, we can distinguish three different cases of the resonant phenomena explaining the observed frequencies.

$\nu_r : \nu_h \sim 3:2$

The observed frequency pattern is given by $\nu_u = \nu_r$, $\nu_m = \nu_h$, $\nu_l = \nu_r - \nu_h$. The value of the spin, given by the frequency ratio, and the humpy frequency are then given by (compare Figs 2 and 3)

$$a_{3:2} = 0.999984, \quad \nu_{h(3:2)} = 590 \frac{M_\odot}{M} \text{ Hz}. \quad (30)$$

Using the condition $\nu_m = \nu_h$, we obtain mass of the black hole to be

$$M = 0.667 \times 10^6 M_\odot. \quad (31)$$

(Note that in this case we have chosen – see Fig. 3 – the value of the spin at the region where the frequency ratio $\nu_r : \nu_h$ starts to be close to the asymptotical value of $\sim 3:2$.)

$\nu_r : \nu_h \sim 2:1$

The observed frequency pattern is given by $\nu_u = \nu_r + \nu_h$, $\nu_m = \nu_r$, $\nu_l = \nu_h$. The value of the spin and the humpy frequency are then given by (compare Figs 2 and 3)

$$a_{2:1} = 0.99925, \quad \nu_{h(2:1)} = 567 \frac{M_\odot}{M} \text{ Hz}. \quad (32)$$

Using the condition $\nu_l = \nu_h$, we obtain mass of the black hole to be

$$M = 1.235 \times 10^6 M_\odot. \quad (33)$$

$\nu_r : \nu_h \sim 3:1$

The observed frequency pattern is given by $\nu_u = \nu_r$, $\nu_m = \nu_r - \nu_h$, $\nu_l = \nu_h$. The value of the spin and the humpy frequency are given by (Figs 2 and 3)

$$a_{3:1} = 0.999984, \quad \nu_{h(3:1)} = 425 \frac{M_\odot}{M} \text{ Hz}. \quad (34)$$

Using the condition $\nu_1 = \nu_h$, we obtain mass of the black hole to be

$$M = 0.926 \times 10^6 M_\odot. \quad (35)$$

However, by analysing data of the orbits of stars moving within 1000 light hours of the Sgr A* black hole, its mass is estimated to be $M \sim 3.6 \times 10^6 M_\odot$, and the error of the estimate is given by (Ghez et al., 2005; Weinberg et al., 2005)

$$2.8 \times 10^6 M_\odot < M < 4.6 \times 10^6 M_\odot. \quad (36)$$

Clearly, the Sgr A* black hole mass predicted by the three simple variants of the EXORM are all completely out of the mass estimates given by relatively precise star-orbit measurements. Therefore, we can conclude that the EXORM cannot be applied to explain the QPOs observed in the Sgr A* black hole candidate. Although we expect a fast rotating black hole in the Galaxy Centre, it is probably not a near-extreme Kerr black hole that sites in Sgr A*.

5 CONCLUDING REMARKS

The extended orbital resonance model with the hypothetical humpy oscillations could be related to the QPO resonant phenomena in both thin Keplerian discs and marginally stable tori orbiting near-extreme Kerr black holes. The non-linear resonance is assumed between oscillations with the humpy frequency and the radial or vertical epicyclic frequency. Both parametric and forced resonance phenomena are possible, therefore, the combinational frequencies are allowed too. Generally, more than two observable oscillations are predicted.

The EXORM can successfully explain all five QPO frequencies observed in the microquasar GRS 1915+105 (Stuchlík et al., 2007d), where a near-extreme black hole with $a \sim 1$ is predicted by spectral X-ray continuum fitting (McClintock et al., 2006). Although Middleton et al. (2006) refer to a substantially lower, intermediate value of the black-hole spin, $a \sim 0.7$, to which the EXORM cannot be applied, the recent analysis by Narayan et al. (2007) and McClintock et al. (2007) demonstrated convincingly that the near-extreme black hole is more probable there, making the predictions of the EXORM still well viable. This model is successfully applied to explain QPOs observed also in the case of the other microquasar XTE J1650–500, and in the near-extreme intermediate-mass Kerr black hole candidate in the system NGC 5408 X-1 (Slaný and Stuchlík, 2007).

On the other hand, the EXORM is not able to explain, in any of its variants, the QPOs observed in the Sgr A* source, i.e., in the Galactic Centre Kerr black hole. The differences in the black hole mass estimated by the EXORM and by analysing the star orbits in vicinity of the black hole are too high to believe that some more exact QPOs measurements could give a solution of this discrepancy. On the other hand, it is worth to note that the Sgr A* QPOs, if true, could be explained within the multiresonance model based on the assumption of strong resonances of oscillation with the orbital and both epicyclic frequencies (Stuchlík et al., 2007a).

The spin estimated in this case is ~ 0.983 , corresponding to a fast rotating, but not near-extreme Kerr black hole.

We can conclude that the EXORM could be considered as a promising model of QPOs in near-extreme Kerr black holes systems, where the oscillations occur in the innermost parts of the accretion disc. The model enables very precise measurements of the black hole parameters, in particular, of the black hole spin since its value is given (usually) by the frequency ratio of the humpy frequency and the radial epicyclic frequency. However, the predictions of the EXORM have to be confronted to the black hole parameter estimates coming from other methods, as those based on the optical phenomena in strong gravitational fields, e.g., the spectral X-ray continuum fitting, the profiled spectral (Fe-K) lines fitting, time delay methods, or by methods based on the orbital motion analysis. The present situation seems to be rather controversial, however, we believe that in future, with developing both the theoretical models and observational techniques, we could be able to understand the accretion phenomena in much deeper detail as compared to the present understanding.

ACKNOWLEDGEMENTS

This work was supported by the Czech grant MSM 4781305903 and by the GAČR grant 202/06/0041 (Z. S.).

REFERENCES

- Abramowicz, M. A., Jaroszyński, M. and Sikora, M. (1978), Relativistic accreting disks, *Astronomy and Astrophysics*, **63**(1–2), pp. 221–224, URL <http://adsabs.harvard.edu/abs/1978A%26A...63..221A>.
- Abramowicz, M. A., Karas, V., Kluźniak, W., Lee, W. and Rebusco, P. (2003), Non-Linear Resonance in Nearly Geodesic Motion in Low-Mass X-Ray Binaries, *Publ. Astronom. Soc. Japan*, **55**(2), pp. 467–471, URL <http://pasj.asj.or.jp/v55/n2/550214/550214-frame.html>.
- Abramowicz, M. A. and Kluźniak, W. (2001), A precise determination of black hole spin in GRO J1655–40, *Astronomy and Astrophysics Lett.*, **374**, pp. L19–L21.
- Abramowicz, M. A., Kluźniak, W., Stuchlík, Z. and Török, G. (2004), Twin peak QPOs frequencies in microquasars and Sgr A*. The resonance and other orbital models, in Hledík and Stuchlík (2004), pp. 1–23.
- Abramowicz, M. A., Miller, J. and Stuchlík, Z. (1993), Concept of radius of gyration in general relativity, *Phys. Rev. D*, **47**(4), pp. 1440–1447, ISSN 1089-4918, URL <http://link.aps.org/abstract/PRD/v47/p1440>.
- Abramowicz, M. A., Nurowski, P. and Wex, N. (1995), Optical reference geometry for stationary and axially symmetric spacetimes, *Classical Quantum Gravity*, **12**(6), pp. 1467–1472, URL <http://www.iop.org/EJ/abstract/0264-9381/12/6/012>.
- Aliev, A. N. and Galtsov, D. V. (1981), Radiation from relativistic particles in non-geodesic motion in a strong gravitational field, *Gen. Relativity Gravitation*, **13**, pp. 899–912.

- Aschenbach, B. (2004), Measuring mass and angular momentum of black holes with high-frequency quasi-periodic oscillations, *Astronomy and Astrophysics*, **425**, pp. 1075–1082, arXiv: [astro-ph/0406545](#).
- Aschenbach, B. (2006), Mass and Angular Momentum of Black Holes: An Overlooked Effect of General Relativity Applied to the Galactic Center Black Hole Sgr A*, *Chinese Astronom. Astrophys.*, **6**, pp. 221–227, updated version of a talk given at the 2005 Frascati Workshop, Vulcano, Italy, May 23–28, arXiv: [astro-ph/0603193](#).
- Aschenbach, B. (2007), Measurement of Mass and Spin of Black Holes with QPOs, *Chinese Astronom. Astrophys.*, accepted for publication, arXiv: [0710.3454](#).
- Aschenbach, B., Grosso, N., Porquet, D. and Predehl, P. (2004), X-ray flares reveal mass and angular momentum of the Galactic Center black hole, *Astronomy and Astrophysics*, **417**, pp. 71–78, arXiv: [astro-ph/0401589](#).
- Bardeen, J. M., Press, W. H. and Teukolsky, S. A. (1972), Rotating black holes: locally nonrotating frames, energy extraction, and scalar synchrotron radiation, *Astrophys. J.*, **178**, pp. 347–369.
- Belloni, T., Méndez, M. and Sánchez-Fernández, C. (2001), The high-frequency QPOs in GRS 1915+105, *Astronomy and Astrophysics*, **372**, pp. 551–556, arXiv: [astro-ph/0104019](#).
- Blaes, O. M., Šrámková, E., Abramowicz, M. A., Kluźniak, W. and Torkelsson, U. (2007), Epicyclic Oscillations of Fluid Bodies. Paper III. Newtonian Non-Slender Torus, *Astrophys. J.*, **665**, pp. 642–653, arXiv: [0706.4483](#), URL <http://adsabs.harvard.edu/abs/2007ApJ...665..642B>.
- Genzel, R., Schödel, R., Ott, T., Eckart, A., Alexander, T., Lacombe, F., Rouan, D. and Aschenbach, B. (2003), Near-infrared flares from accreting gas around the supermassive black hole at the Galactic Centre, *Nature*, **425**, pp. 934–937, arXiv: [astro-ph/0310821](#).
- Ghez, A. M., Salim, S., Hornstein, S. D., Tanner, A., Lu, J. R., Morris, M., Becklin, E. E. and Duchêne, G. (2005), Stellar Orbits around the Galactic Center Black Hole, *Astrophys. J.*, **620**, pp. 744–757, arXiv: [astro-ph/0306130](#).
- Hledík, S. and Stuchlík, Z., editors (2004), *Proceedings of RAGtime 4/5: Workshops on black holes and neutron stars, Opava, 14–16/13–15 October 2002/2003*, Silesian University in Opava, Opava, ISBN 80-7248-242-4.
- Kato, S. (2001), Trapping of Non-Axisymmetric g-Mode Oscillations in Thin Relativistic Disks and kHz QPOs, *Publ. Astronom. Soc. Japan*, **53**, pp. L37–L39.
- Kato, S. (2004), Mass and Spin of GRS 1915+105 Based on a Resonance Model of QPOs, *Publ. Astronom. Soc. Japan*, **56**(5), pp. L25–L28.
- Kluźniak, W. and Abramowicz, M. A. (2001), Strong-field gravity and orbital resonance in black holes and neutron stars – kHz quasi-periodic oscillations (QPO), *Acta Phys. Polon. B*, **32**, pp. 3605–3612.
- Kozłowski, M., Jaroszyński, M. and Abramowicz, M. A. (1978), The analytic theory of fluid disks orbiting the Kerr black hole, *Astronomy and Astrophysics*, **63**(1–2), pp. 209–220, URL <http://adsabs.harvard.edu/abs/1978A%26A...63..209K>.
- McClintock, J. E., Narayan, R. and Shafee, R. (2007), Estimating the Spins of Stellar-Mass Black Holes, in M. Livio and A. Koekemoer, editors, *Black Holes*, volume 707, Cambridge University Press, Cambridge, in press, to appear in 2008, arXiv: [0707.4492v1](#).
- McClintock, J. E. and Remillard, R. A. (2004), Black Hole Binaries, in W. H. G. Lewin and M. van der Klis, editors, *Compact Stellar X-Ray Sources*, Cambridge University

- Press, Cambridge, arXiv: [astro-ph/0306213](#).
- McClintock, J. E., Shafee, R., Narayan, R., Remillard, R. A., Davis, S. W. and Li, L. (2006), The Spin of the Near-Extreme Kerr Black Hole GRS 1915+105, *Astrophys. J.*, **652**(2), pp. 518–539, arXiv: [astro-ph/0606076](#).
- Middleton, M., Done, C., Gierliński, M. and Davis, S. W. (2006), Black hole spin in GRS 1915+105, *Monthly Notices Roy. Astronom. Soc.*, **373**(3), pp. 1004–1012, arXiv: [astro-ph/0601540v2](#).
- Morgan, E. H., Remillard, R. A. and Greiner, J. (1997), RXTE Observation of GRS 19115+105, *Astrophys. J.*, **482**, pp. 993–1010.
- Narayan, R., McClintock, J. E. and Shafee, R. (2007), Estimating the Spins of Stellar-Mass Black Holes by Fitting Their Continuum Spectra, in Y. F. Yuan, X. D. Li and D. Lai, editors, *Astrophysics of Compact Objects*, AIP, to appear, arXiv: [0710.4073v1](#).
- Remillard, R. A. (2005), X-ray spectral states and high-frequency QPOs in black hole binaries, *Astronom. Nachr.*, **326**(9), pp. 804–807, arXiv: [astro-ph/0510699](#).
- Remillard, R. A. and McClintock, J. E. (2006), X-Ray Properties of Black-Hole Binaries, *Annual Review of Astronomy and Astrophysics*, **44**(1), pp. 49–92, arXiv: [astro-ph/0606352](#).
- Rezzolla, L., Yoshida, S., Maccarone, T. J. and Zanotti, O. (2003), A new simple model for high-frequency quasi-periodic oscillations in black hole candidates, *Monthly Notices Roy. Astronom. Soc.*, **344**(3), pp. L37–L41.
- Slaný, P. and Stuchlík, Z. (2007), Extended orbital resonance model applied to QPOs observed in three near-extreme Kerr black hole candidate systems, pp. 253–261, this volume.
- Šrámková, E. (2005), Epicyclic oscillation modes of a Newtonian, non-slender torus, *Astronom. Nachr.*, **326**(9), pp. 835–837.
- Stella, L. and Vietri, M. (1998), Lense–Thirring Precession and Quasi-periodic Oscillations in Low-Mass X-Ray Binaries, *Astrophys. J. Lett.*, **492**, pp. L59–L62, arXiv: [astro-ph/9709085](#).
- Stella, L. and Vietri, M. (1999), kHz Quasiperiodic Oscillations in Low-Mass X-Ray Binaries as Probes of General Relativity in the Strong-Field Regime, *Phys. Rev. Lett.*, **82**(1), pp. 17–20.
- Strohmayer, T. E. (2001), Discovery of a Second High Frequency QPO from the Microquasar GRS 1915+105, *Astrophys. J.*, **554**, pp. L169–L172.
- Stuchlík, Z., Kotrlová, A. and Török, G. (2007a), Multi-resonance models of QPOs, pp. 363–419, this volume.
- Stuchlík, Z., Slaný, P. and Török, G. (2004), Marginally stable thick discs with gradient inversion of orbital velocity measured in locally non-rotating frames: A mechanism for excitation of oscillations in accretion discs?, in Hledík and Stuchlík (2004), pp. 239–256.
- Stuchlík, Z., Slaný, P. and Török, G. (2006a), Humpy LNRF-velocity profiles in accretion discs orbiting rapidly rotating Kerr black holes: a possible relation to QPOs, in T. Belloni, editor, *Proceedings of the Sixth Microquasar Workshop – Microquasars and Beyond: From Binaries To Galaxies, Como, Italy, 18–22 September, 2006*, p. PoS(MQW6)095, Como, Italy, URL http://pos.sissa.it/archive/conferences/033/095/MQW6_095.pdf.
- Stuchlík, Z., Slaný, P. and Török, G. (2006b), Toroidal LNRF-velocity Profiles in Thick Accretion Discs Orbiting Rapidly Rotating Kerr Black Holes, in J.-M. Alimi and A. Fzfa, editors, *Albert Einstein Century International Conference, Paris, France, 18–22 July*

- 2005, volume 861, pp. 778–785, AIP, Melville, New York.
- Stuchlík, Z., Slaný, P. and Török, G. (2007b), Humpy LNRF-velocity profiles in accretion discs orbiting almost extreme Kerr black holes – A possible relation to quasi-periodic oscillations, *Astronomy and Astrophysics*, **463**(3), pp. 807–816, arXiv: [astro-ph/0612439](#).
- Stuchlík, Z., Slaný, P. and Török, G. (2007c), Humpy LNRF-velocity profiles in accretion discs orbiting rapidly rotating Kerr black holes and a possible relation to epicyclic oscillations, in V. Karas and G. Matt, editors, *Black Holes from Stars to Galaxies – Across the Range of Masses*, volume 238 of *Proceedings of IAU Symposium*, pp. 459–460, International Astronomical Union, Cambridge University Press, Cambridge, UK, ISSN 1743-9213.
- Stuchlík, Z., Slaný, P. and Török, G. (2007d), LNRF-velocity hump-induced oscillations of a Keplerian disc orbiting near-extreme Kerr black hole: A possible explanation of high-frequency QPOs in GRS 1915+105, *Astronomy and Astrophysics*, **470**(2), pp. 401–404, arXiv: [0704.1252v2](#).
- Stuchlík, Z., Slaný, P., Török, G. and Abramowicz, M. A. (2005), The Aschenbach effect: unexpected topology changes in motion of particles and fluids orbiting rapidly rotating Kerr black holes, *Phys. Rev. D*, **71**, p. 024037 (9), arXiv: [gr-qc/0411091](#).
- Török, G. (2005), QPOs in microquasars and Sgr A*: measuring the black hole spin, *Astronom. Nachr.*, **326**(9), pp. 856–860, arXiv: [astro-ph/0510669](#).
- Török, G., Abramowicz, M. A., Kluźniak, W. and Stuchlík, Z. (2005), The orbital resonance model for twin peak kHz quasi periodic oscillations in microquasars, *Astronomy and Astrophysics*, **436**(1), pp. 1–8, arXiv: [astro-ph/0401464](#).
- Török, G., Abramowicz, M. A., Kluźniak, W. and Stuchlík, Z. (2006), A non-linear resonance model for the black hole and neutron star QPOs: theory supported by observations, to appear in Proceedings of the Albert Einstein Century International Conference, arXiv: [astro-ph/0603847](#).
- Török, G. and Stuchlík, Z. (2005a), Epicyclic frequencies of Keplerian motion in Kerr spacetimes, in S. Hledík and Z. Stuchlík, editors, *Proceedings of RAGtime 6/7: Workshops on black holes and neutron stars, Opava, 16–18/18–20 September 2004/2005*, pp. 315–338, Silesian University in Opava, Opava, ISBN 80-7248-334-X.
- Török, G. and Stuchlík, Z. (2005b), Radial and vertical epicyclic frequencies of Keplerian motion in the field of Kerr naked singularities. Comparison with the black hole case and possible instability of naked singularity accretion discs, *Astronomy and Astrophysics*, **437**(3), pp. 775–788, arXiv: [astro-ph/0502127](#).
- van der Klis, M. (2000), Millisecond Oscillations in X-ray Binaries, *Annual Review of Astronomy and Astrophysics*, **38**, pp. 717–760, arXiv: [astro-ph/0001167](#).
- Weinberg, N. N., Milosavljević, M. and Ghez, A. M. (2005), Astrometric Monitoring of Stellar Orbits at the Galactic Center with a Next Generation Large Telescope, in P. K. Seidelmann and A. K. B. Monet, editors, *Astrometry in the Age of the Next Generation of Large Telescopes*, volume 338 of *ASP Conf. Series*, p. 252, ASP, arXiv: [astro-ph/0512621v2](#).